THE JOURNAL OF BIOLOGICAL CHEMISTRY VOL. 285, NO. 16, pp. 12133–12139, April 16, 2010

Reaction Mechanism and Molecular Basis for Selenium/Sulfur Discrimination of Selenocysteine Lyase*[S]

Received for publication, November 12, 2009, and in revised form, February 13, 2010 Published, JBC Papers in Press, February 17, 2010, DOI 10.1074/jbc.M109.084475

Rie Omi[‡1], Suguru Kurokawa[‡1], Hisaaki Mihara[§2], Hideyuki Hayashi[¶], Masaru Goto[‖], Ikuko Miyahara[‖], Tatsuo Kurihara[‡], Ken Hirotsu[‖3], and Nobuyoshi Esaki[‡4]

From the [‡]Institute for Chemical Research, Kyoto University, Uji, Kyoto 611-0011, Japan, the [‖]Department of Chemistry, Graduate School of Science, Osaka City University, Osaka 558-8585, Japan, the [§]Department of Biotechnology, Institute of Science and Engineering, College of Life Sciences, Ritsumeikan University, Kusatsu, Shiga 525-8577, Japan, and the [¶]Department of Biochemistry, Osaka Medical College, 2-7 Daigakumachi, Takatsuki 569-8686, Japan

Selenocysteine lyase (SCL) catalyzes the pyridoxal 5′-phosphate-dependent removal of selenium from L-selenocysteine to yield L-alanine. The enzyme is proposed to function in the recycling of the micronutrient selenium from degraded selenoproteins containing selenocysteine residue as an essential component. The enzyme exhibits strict substrate specificity toward L-selenocysteine and no activity to its cognate L-cysteine. However, it remains unclear how the enzyme distinguishes between selenocysteine and cysteine. Here, we present mechanistic studies of selenocysteine lyase from rat. ESI-MS analysis of wild-type and C375A mutant SCL revealed that the catalytic reaction proceeds via the formation of an enzyme-bound selenopersulfide intermediate on the catalytically essential Cys-375 residue. UV-visible spectrum analysis and the crystal structure of SCL complexed with L-cysteine demonstrated that the enzyme reversibly forms a nonproductive adduct with L-cysteine. Cys-375 on the flexible loop directed L-selenocysteine, but not L-cysteine, to the correct position and orientation in the active site to initiate the catalytic reaction. These findings provide, for the first time, the basis for understanding how trace amounts of a selenium-containing substrate is distinguished from excessive amounts of its cognate sulfur-containing compound in a biological system.

Selenium is an essential trace element required for the normal function of mammals (1). It is similar to sulfur in its chemical properties and needs to be discriminated biologically from abundant sulfur during its metabolism. During the synthesis of selenoproteins, selenium is specifically incorporated into selenocysteyl-tRNA^{Sec} and eventually into the specific position of the nascent polypeptide chains as directed by the UGA codon (2). The specific synthesis of selenocysteyl-tRNA^{Sec} from seryl-tRNA^{Sec} and selenide involves coordinated sequential reactions catalyzed by selenophosphate synthetase (3, 4), seryl-tRNA kinase (5), and selenocysteine synthase (6, 7). However, the mechanism underlying selenium-specific substrate recognition in these enzymes remains unknown.

The most common selenium source in normal foods is selenocysteine and selenomethionine in proteins (8). Previous studies suggest that selenomethionine is transformed to selenocysteine through the trans-selenation pathway (9, 10). Specific cleavage of selenocysteine by selenocysteine lyase (SCL)[5] is thought to be the critical metabolic step for the recycling of selenocysteine, which is formed by proteolytic degradation of selenoproteins.

SCL is a pyridoxal 5′-phosphate (PLP) enzyme that catalyzes the removal of selenium from L-selenocysteine to yield L-alanine. In previous studies, we identified and characterized SCL from pig liver (11) and *Citrobacter freundii* (12) as the first enzyme that discriminately acts on a selenium-containing compound but not on its cognate sulfur analog. The cDNA cloning of mouse SCL (13) revealed that SCL belongs to subgroup V in fold type I of aminotransferases (14). Among them, overall sequence similarity (~30%) is found between mammalian SCL and cysteine desulfurases (13).

SCL and cysteine desulfurase catalyze the same type of reaction, namely the removal of selenium or sulfur from selenocysteine or cysteine to yield alanine. Although bacterial cysteine desulfurases exhibit activity to both cysteine and selenocysteine (15), SCL shows significant specificity to selenocysteine. Mechanistic and crystal structure studies showed that the catalytic reaction of cysteine desulfurase involves the formation of sulfane sulfur in the form of a cysteine persulfide in the active site of the enzyme (16–18). Sulfur transfer from the persulfide to a

* This work was supported in part by Grant-in-aid for Scientific Research on Priority Areas (B) 19370040 (to N. E.) from the Ministry of Education, Culture, Sports, Science, and Technology of Japan, by Grant-in-aid for Encouragement of Young Scientists 21780094 (to H. M.) from the Japan Society for the Promotion of Science, by the National Project on Protein Structural and Functional Analyses, and by a grant-in-aid from the Ministry of Education, Culture, Sports, Science and Technology of Japan (21st Century COE on Kyoto University Alliance for Chemistry) (to N. E.).

The atomic coordinates and structure factors (codes 3A9X, 3A9Y, and 3A9Z) have been deposited in the Protein Data Bank, Research Collaboratory for Structural Bioinformatics, Rutgers University, New Brunswick, NJ (http://www.rcsb.org/).

[S] The on-line version of this article (available at http://www.jbc.org) contains supplemental Figs. S1–S4 and Experimental Procedures.

[1] Both authors contributed equally to this work.

[2] To whom correspondence may be addressed: Dept. of Biotechnology, Institute of Science and Engineering, College of Life Sciences, Ritsumeikan University, Kusatsu, Shiga 525-8577, Japan. Tel.: 81-775-61-2732; Fax: 81-775-61-2659; E-mail: mihara@fc.ritsumei.ac.jp.

[3] To whom correspondence may be addressed: RIKEN Spring-8 Center, Harima Institute, 1-1-1 Kouto, Sayo, Hyogo 679-5148, Japan. Tel.: 81-791-58-2891; Fax: 81-791-58-2892; E-mail: hirotsu@spring8.or.jp.

[4] Recipient of 2009 Humboldt Research Award. To whom correspondence may be addressed: Institute for Chemical Research, Kyoto University, Uji, Kyoto 611-0011, Japan. Tel.: 81-774-38-3240; Fax: 81-774-38-3248; E-mail: esakin@SCL.kyoto-u.ac.jp.

[5] The abbreviations used are: SCL, selenocysteine lyase; PLP, pyridoxal 5′-phosphate; ESI-MS, electrospray ionization mass spectrometry; PDB, Protein Data Bank.

cysteine residue of its partner proteins, such as IscU (19), ThiI (20), TusA (21), and SufE (22, 23), is associated with direct protein-protein interaction, thereby ensuring the specific delivery of the persulfide sulfur to eventual target molecules, such as an iron-sulfur cluster, thiamine, and thiolated nucleosides, without nonspecific spreading of reactive sulfur in the cell (24). Although SCL has a conserved cysteine residue at the position corresponding to the persulfide-forming cysteine residue of cysteine desulfurase, its role in the catalytic function of the enzyme has not been established.

Here, we investigate the mechanism of rat SCL. Site-directed mutagenesis and ESI-MS studies using wild-type and C375A mutant of SCL show that Cys-375 is essential for the activity of SCL as the site for cysteine selenopersulfide formation. UV-visible spectrum analysis and crystal structure of SCL complexed with L-cysteine in a non-productive adduct form shows the structural basis for discrimination between selenocysteine and cysteine by the enzyme. UV-visible spectrum analysis also shows that loss of Cys-375 resulted in the formation of a non-productive adduct with selenocysteine, suggesting that Cys-375 serves as a guide to direct the substrate in an appropriate orientation for the catalytic reaction.

EXPERIMENTAL PROCEDURES

Materials—L-Selenocystine and L-cysteine were purchased from Sigma Aldrich. Selenopropionate was synthesized as described in supplemental Experimental Procedures. Oligonucleotides were synthesized by Hokkaido System Science (Sapporo, Japan). Restriction and DNA modification enzymes were purchased from New England Biolabs (Beverly, MA), Takara Shuzo (Kyoto, Japan) and Toyobo (Osaka, Japan). All other chemicals were analytical grade reagents.

Gene Expression and Purification of SCL—cDNA for the full-length SCL protein of *Rattus norvegicus* (GenBank^{TM}/EMBL accession number NM_001007755) was cloned by PCR using the primers 5′-AGCGATCAGGCATATGGACGTGGCGCGGAATGGC-3′ and 5′-CCGGAATTCCTAGACCGGGCTTCCAGCTGGTTC-3′. PCR products were cloned into the NdeI and EcoRI sites of pET21a(+) for heterologous expression in *Escherichia coli* Rosetta(DE3). The *E. coli* cells harboring the expression plasmid were grown in an LB medium containing 50 μg/ml ampicillin at 28 °C for 16 h and were harvested by centrifugation. A Tris-HCl buffer (10 mM) (pH 7.4) containing 0.1 mM phenylmethylsulfonyl fluoride and 1 mM EDTA was used as the standard buffer. The cells were disrupted by sonication. The cell debris was removed by centrifugation, and the supernatant solution was applied to a Q-Sepharose column (5 × 5 cm). After the column was washed, the enzyme was eluted with a 1.0-liter linear gradient of 0–0.5 M NaCl in the buffer. The fractions containing SCL were pooled, mixed with an equal volume of standard buffer containing 2.0 M ammonium sulfate, and applied to a Butyl-Toyopearl column (3 × 15 cm). After the column was washed, the enzyme was eluted with a 1.0-liter linear gradient of 1.0–0.6 M ammonium sulfate in the buffer. The enzyme fractions were concentrated with Centriprep YM-30 (Millipore, Bedford, MA) and stored at −80 °C until use without significant inactivation. Purification of the C375A mutant of SCL was performed in the same manner as described for the wild-type enzyme.

Site-directed Mutagenesis—Site-directed mutagenesis was performed by using the QuikChange site-directed mutagenesis kit (Stratagene, La Jolla, CA). The mutagenic oligonucleotides used were 5′-ATCCGAGTGGGCTGAAGCTCC-3′ and 5′-GGAGCTTCAGCCCACTCGGAT-3′.

Enzyme Assay and Kinetic Analysis—SCL activity was assayed by the determination of selenide with lead acetate as described previously (25, 26). Protein was determined using the CBB protein assay (Nacalai Tesque, Kyoto, Japan) with bovine serum albumin as a standard.

ESI-MS Sample Preparation and Measurements—Samples of wild-type SCL and the C375A mutant for ESI-MS analysis were prepared under a nitrogen atmosphere in a glove box (Miwa, Osaka, Japan) at room temperature. SCL (230 μM) was incubated with L-selenocysteine (70 μM) in a 50 mM Tris-HCl buffer (pH 7.0) and immediately separated with a MicroBioSpin 6 column (Bio-Rad). The desalted enzyme was introduced at a flow rate of 18 μl/min into a PE Sciex API 2000 single quadrupole mass spectrometer equipped with an electrospray ionization source (PE-Sciex, Thornhill, ON, Canada). The mass spectrometer scanned from $m/z = 800$ to $m/z = 1800$ with a 2.0 ms dwell time and a 0.2 m/z step size.

Crystallization and Data Collection—The purified enzyme was dialyzed against 10 mM HEPES-NaOH (pH 7.5). SCL crystals were grown by the hanging-drop vapor-diffusion method at 297 K. A 2 μl droplet of a 35 mg·ml^{-1} protein solution mixed with the same amount of reservoir solution was equilibrated at 293 K against a 500 μl reservoir solution (100 mM citrate buffer pH 4.7 and 1.5 M ammonium dihydrogen phosphate). The native crystals appeared within 2 weeks of incubation and grew to maximum dimensions of 0.3 × 0.3 × 0.1 mm. The crystals (pH 4.7) were transferred to the reservoir solution adjusted to pH 8.0 using 1.5 M di-ammonium hydrogen phosphate instead of ammonium dihydrogen phosphate, to produce the native crystals at pH 8.0. Crystals of SCL·L-cysteine and SCL·selenopropionate were obtained at 293 K by soaking the native crystals in the reservoir solution adjusted to pH 8.0. These crystals are isomorphous with the orthorhombic space group $P2_12_12_1$, average unit cell parameters $a = 55.0$, $b = 101.9$, $c = 197.3$ Å. Assuming two monomers in the asymmetric unit, the Matthews coefficient (V_M) value was calculated to be 2.96 Å^3 Da^{-1}, indicating an estimated solvent content of 58.3% in the unit cell (27).

Data collection was performed at 100 K using a wavelength of 1.00 Å from the synchrotron-radiation source and an ADSC Quantum CCD Camera. X-ray diffraction data sets for the unliganded SCL (pH 8.0) were collected to 2.0 Å resolution on the BL5A station at the Photon Factory, KEK (Tsukuba, Japan). X-ray diffraction data sets for the SCL·L-cysteine crystal and the SCL·selenopropionate crystal were collected to 1.85 and 1.55 Å resolution on the BL41XU and the BL38B2 station, respectively, at SPring8 (Hyogo, Japan). Data were processed using DENZO/SCALEPACK (28). Data collection statistics are presented in Table 1.

Structure Determination and Refinement—The structure of the unliganded SCL (pH 8.0) was solved by the molecular

replacement method with the program AMoRe (29) using the IscS structure (PDB ID: 1P3W) as the search model. The modeling of the polypeptide chain was performed using program O (30), and the structure was refined with program CNS (31). Water molecules were picked up on the basis of the peak heights (1.5 σ) and distance criteria (4.0 Å from protein and solvent) from the sigma-weighted $2F_o - F_c$ map.

TABLE 1
Data collection and refinement statistics

	SCL	SCL·L-cysteine	SCL·selenopropionate
Diffraction data			
Wavelength (Å)	1.0	1.0	1.0
Resolution (Å)	2.00	1.85	1.55
Unique no. of reflections	69817	86205	159678
Completeness (%)	91.8 (85.0)[b]	90.3 (85.2)[b]	98.7 (94.4)[b]
R_{merge} (%)[a]	4.3 (29.9)[b]	5.8 (25.6)[b]	4.4 (29.9)[b]
I/σ(I)	28.3	38.2	36.4
Refinement			
Resolution limits (Å)	20.0–2.00	20.0–1.85	20–1.55
R_{factor} (%)	19.7 (25.7)[b]	18.7 (24.1)[b]	18.7 (23.4)[b]
R_{free} (%)	23.6 (27.4)[b]	21.1 (27.5)[b]	20.9 (26.4)[b]
Deviations			
Bond length (Å)	0.022	0.007	0.029
Bond angles (deg)	2.1	1.3	2.4
Mean B factor			
Main chain atoms (Å^2)	32.1	22.0	21.1
Side-chain atoms (Å^2)	33.4	23.6	22.7
Water atoms (Å^2)	36.3	31.1	31.3
Hetero atoms (Å^2)	PLP 31.1	PLP 16.7	PLP 17.0
	PO_4 61.0	PO4 37.4	PO4 34.6
		GOL 45.3	GOL 34.4
		CYS 21.8	SLP 10.2
Ramachandran plot			
Favored	92.7	91.5	92.3
Additional allowed	7.3	8.5	7.7
Generously allowed	0.0	0.0	0.0
Disallowed	0.0	0.0	0.0

[a] $R_{merge} = \Sigma_{hkl} \Sigma_i |I_{hkl,i} - <I_{hkl}>| / \Sigma_{hkl} \Sigma_i I_{hkl,i}$, where I = observed intensity and $<I>$ = average intensity for multiple measurements.
[b] The values in the parentheses are for the highest resolution shells (2.01–2.00, 1.85–1.86, 1.55–1.56 Å) in SCL, SCL·L-cysteine, and SCL·selenopropionate, respectively.

The water molecules whose thermal factors were above the maximum thermal factor of the main chain after refinement were removed from the list. Model building and refinement cycles resulted in an R_{factor} of 0.197 and an R_{free} of 0.236% at 2.0 Å resolution, calculated for 69817 reflections. The same refinement procedure was applied to SCL·L-cysteine and SCL·selenopropionate but using the coordinates of the native enzyme as the initial model. Refinement cycles resulted in an R_{factor} of 0.187 and 0.211 and R_{free} of 0.187 and 0.209 for SCL·L-cysteine and SCL·selenopropionate, respectively. Structure diagrams were drawn using MOLSCRIPT (32), POVSCRIPT+ (33), and PyMol (34).

RESULTS

Purification and Properties of Rat SCL—Because our attempt to obtain crystals of SCL cloned from mouse liver (13) was unsuccessful, we constructed an expression system for rat SCL. The recombinant SCL was purified to homogeneity. Steady-state kinetic analysis revealed that V_{max} and K_m values for L-selenocysteine were 26 μmol·min^{-1}·mg^{-1} and 5.5 mM, respectively (supplemental Fig. S1). The enzyme showed no detectable activity toward L-cysteine (examined at 5–50 mM). An inhibition study showed that L-cysteine is a competitive inhibitor of the enzyme with K_i = 9.6 mM (supplemental Fig. S1). Thus, the fundamental properties SCL are similar to those reported for the enzymes from pig (11) and mouse (13).

Role of Cys-375—SCL has a conserved cysteine residue that corresponds to the persulfide-forming cysteine residue in cysteine desulfurases (supplemental Fig. S2) (16, 35). To investigate the role of the conserved cysteine residue in SCL, we prepared a mutant SCL protein (C375A) in which Cys-375 was replaced by an alanine residue. The purified C375A mutant exhibited no activity to L-selenocysteine, suggesting that Cys-375 is a catalytically essential residue of the enzyme similar to the conserved catalytic cysteine residue of cysteine desulfurases (35).

ESI-MS Analysis of Enzyme-bound Selenopersulfide Intermediate—To further elucidate the catalytic role of Cys-375, the formation of an SCL-bound selenopersulfide intermediate was assessed by ESI-MS analysis. The observed masses of the wild-type (47,273 Da) and the mutant (47,243 Da) SCL were consistent with their masses calculated from the amino acid sequences (47,261 and 47,229 Da, respectively) within acceptable error of ESI-MS measurement (<0.1%) (Fig. 1, *A* and *D*). Incubation of the wild-type SCL with L-selenocysteine resulted in the formation of a new species with a mass of [M + 80] (Fig. 1*C*). In contrast, incubation with L-cysteine resulted in no formation of such species (Fig. 1*B*). The data suggest

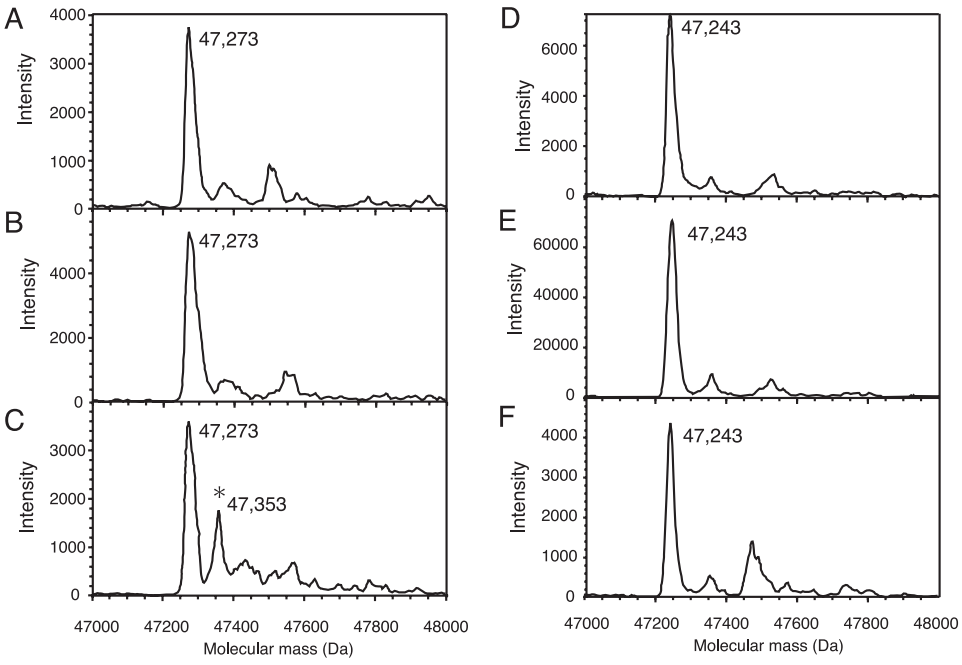

FIGURE 1. **Deconvoluted ESI-mass spectra of SCL.** Wild-type SCL (*A–C*) or the C375A mutant enzyme (*D–F*) was incubated with L-cysteine (*B*, *E*), L-selenocysteine (*C*, *F*), or none (*A*, *D*) and analyzed by ESI-mass spectrometer as described under "Experimental Procedures." The peak at the mass of 47,353 for the [M + 80] species that corresponds to the selenopersulfide form of SCL (SCL-S-Se$^-$) is indicated by an *asterisk*.

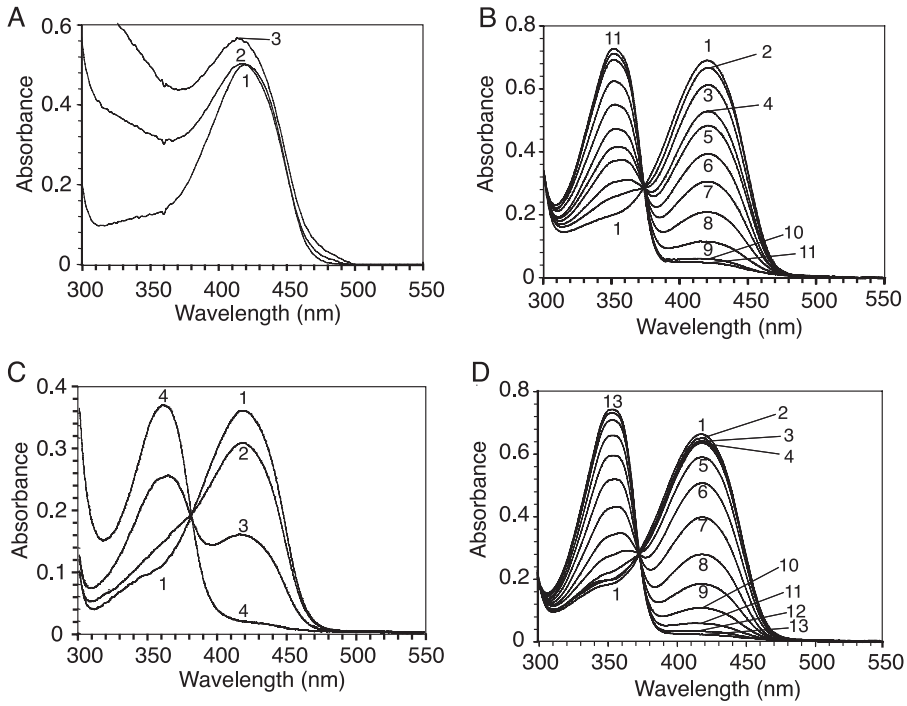

FIGURE 2. **UV-visible spectroscopic analysis of SCL.** *A*, absorption spectra of wild-type SCL incubated with various concentrations (0, 15, and 30 μM, indicated by *lines 1*, *2*, and *3*, respectively) of L-selenocysteine. *B*, absorption spectra of wild-type SCL incubated with various concentrations (0, 0.027, 0.1, 0.26, 0.6, 1.25, 2.5, 5, 10, 20, and 40 mM, indicated by *lines 1–11*, respectively) of L-cysteine. *C*, absorption spectra of the C375A mutant incubated with various concentration (0, 1.5, 15, and 30 μM, indicated by *lines 1–4*) of L-selenocysteine. *D*, absorption spectra of the C375A mutant incubated with various concentrations (0, 0.0024, 0.0073, 0.027, 0.1, 0.26, 0.6, 1.25, 2.5, 5, 10, 20, and 40 mM, indicated by *lines 1–13*) of L-cysteine. Absorption spectra of SCL were recorded with a Shimadzu UV-visible spectrophotometer (UV-2450, Shimadzu, Kyoto, Japan) at pH 7.0.

that the [M + 80] species corresponds to a selenium-bound form of SCL. The C375A mutant incubated with L-selenocysteine or L-cysteine did not produce the [M + 80] molecule (Fig. 1, *E* and *F*), indicating that selenium eliminated from L-selenocysteine is bound to Cys-375 of the enzyme in the form of a cysteine selenopersulfide intermediate (SCL-S-Se$^-$).

UV-visible Spectrum Analysis—SCL shows an absorption maximum at 416 nm, which is characteristic of the internal aldimine form of PLP enzymes. Incubation of SCL with L-selenocysteine resulted in a broad increase in the absorbance at ~420 nm (Fig. 2*A*). In contrast, the addition of L-cysteine to the enzyme caused a significant decrease in the absorption peak at 416 nm, concomitantly with the increase in that at 350 nm (Fig. 2*B*). The incubation with D-cysteine, D-selenocysteine, or 2-mercaptoethanol also resulted in an absorption peak shift from 416 nm to 330–340 nm in the same manner as observed in the enzyme incubated with L-cysteine (data not shown). These results indicate that L-cysteine, D-cysteine, D-selenocysteine, and 2-mercaptoethanol can enter the active site of the enzyme to affect the absorption properties of the PLP moiety even though they do not serve as a substrate of the enzyme. Interestingly, the C375A mutant enzyme incubated with L-selenocysteine or L-cysteine also showed a peak shift from 416 nm to 350 nm (Fig. 2, *C* and *D*). These results indicate that Cys-375 is essential for the proper capture of the substrate L-selenocysteine.

Overall Structure—The overall structure of SCL is shown in Fig. 3*A*. The polypeptide chain is folded into a dimeric form with each subunit consisting of the small (from N terminus to Leu-30 and from Thr-306 to the C terminus) and large (from Glu-31 to Glu-305) domains. The small domain has an α/β structure which consists of a two-stranded parallel β-sheet, three-stranded antiparallel β-sheet, and six helices (supplemental Fig. S3*B*). The large domain exhibits a typical α/β structure in which seven parallel β-strands (S2–S8), except for S8 form an open twisted β-sheet as a core surrounded by six α-helices from the solvent side and two α-helices from the protein side. The seven-stranded β-sheet forms the base of the active site that binds the coenzyme PLP, and is characteristic of PLP-dependent fold type I enzyme (14, 36). The molecule has two active site cavities around a molecular 2-fold axis. Each cavity is located at the domain interface of one subunit and at the subunit interface.

The program DALI (37) was used to detect the enzymes possessing three-dimensional structures most similar to that of the unliganded SCL from among PLP-dependent fold type I enzymes in the Protein Data Bank data base. The highest Z scores were calculated to be 62.4 for human SCL (an as yet unpublished structure, PDB 2HDY), 49.5 for *E. coli* IscS (38), 48.2 for *Thermotoga maritima* NifS-like protein (39), 40.6 for *Synechocystis* sp. PCC 6803 SufS (40), 38.9 for *E. coli* CsdB (17, 18), 35.2 for *Synechocystis* cystine C-S lyase (41), and 30.5 for *Pseudomonas fluorescens* kynureninase (42). This result shows that the structure of SCL is quite similar to that of human SCL, and more similar to those of group I cysteine desulfurases (IscS and NifS-like protein) than those of group II cysteine desulfurases (SufS and CsdB) (35, 43) (Fig. 3*B*).

SCL changes its overall conformation from the open form to the closed form by a 3.8° rotation of the small domain as a rigid body upon binding of cysteine to the active site crevice to form the cofactor-cysteine complex (Fig. 3*A*). In addition to the rigid body rotation of the small domain, the cysteine binding induces the local conformational change of the extended lobe (the small domain residues from Ser-374 to Ile-392). The extended lobe of SCL in the unliganded open form was disordered and was not located on the electron density map. In contrast, the lobe in the liganded closed form was ordered to form the helix 11 (3_{10} helix)–loop–α-helix 12-loop structure which covers the active site as a lid. In contrast to SCL, the open-closed conformational change on ligand binding was not observed in cysteine desulfurases (17, 18, 38, 39, 44) (see *Open-Closed Conformational Change* in "Discussion").

Active Site Structure of SCL·L-Cysteine Complex—PLP is located at the bottom of the active site pocket formed at the

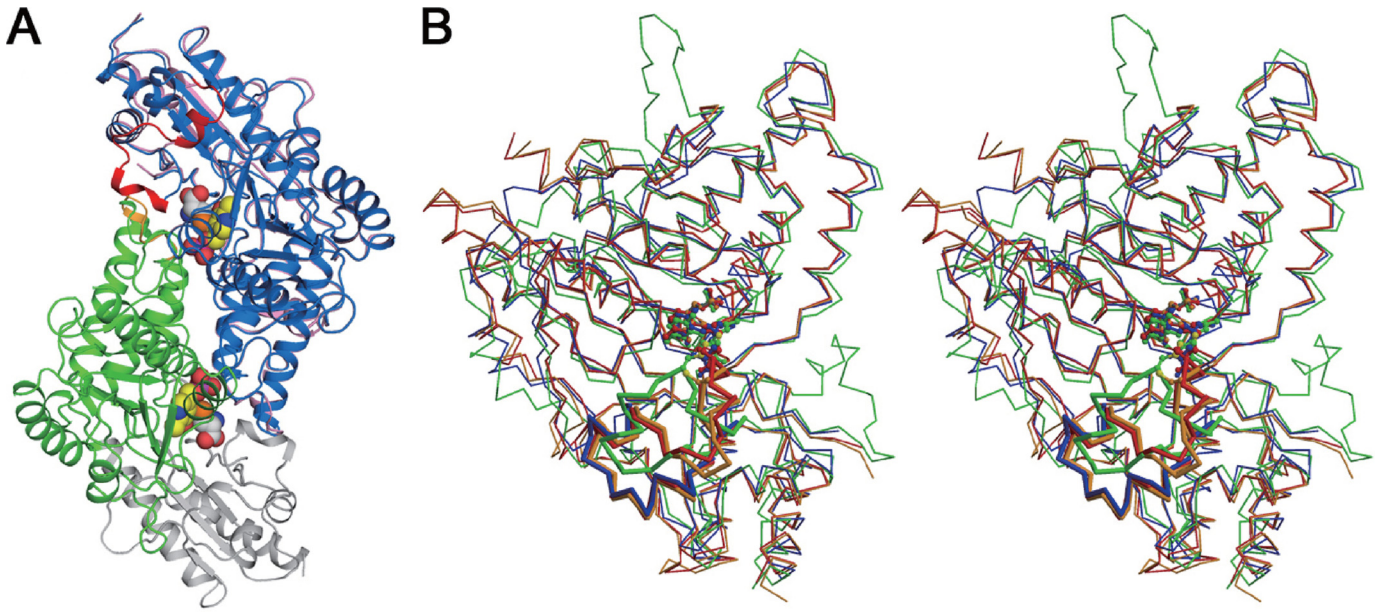

FIGURE 3. **Overall structure of SCL.** *A*, a dimeric form viewed down the crystallographic 2-fold axis. The upper half of the molecules is the superimposition of one subunit in the liganded closed form onto that in the unliganded open form by least-squares fitting of Cα atoms in the large domain. The open form is *pink*, and the closed form is *blue* with a *red* extended lobe. The lower half of the molecule represents the other subunit in the closed form. The small domain, the large domain, and the N-terminal loop are drawn in *gray*, *green*, and *orange*, respectively. The coenzyme PLP and L-cysteine located in the domain interface are represented by CPK models. The extended lobe in the open form of SCL is disordered and, therefore, not shown in the model. *B*, superpositioning of Cα atoms of SCL onto those of cysteine desulfurases. SCL complexed with L-cysteine, human SCL, *T. maritima* NifS-like protein complexed with L-cysteine (PDB ID: 1ECX), and *E. coli* CsdB complexed with L-propargylglycine (1I29) are presented in *red*, *orange*, *blue*, and *green*, respectively. The extended lobes are shown in *thick lines*. The PLP moieties, bound ligands, and active site lysine and cysteine residues are represented by *stick models*. A part of the extended lobe of *T. maritima* NifS-like protein is disordered and not shown in the model.

subunit interface and the domain interface (Fig. 4*A*). The side chain Sγ atom of the bound cysteine, but not the α-amino group, makes a covalent bond with the C4′ atom of PLP. The residual electron density of the Sγ atom of the bound cysteine was so close to C4′ of PLP that the Sγ atom made a covalent bond with C4′ (supplemental Fig. S3*C*). When the C4′-N bond between PLP and Lys-247 was refined as a double bond (Schiff base), C4′-N linkage deviated from the corresponding electron density compared with the Schiff base in the unliganded form. The C4′-N and C4′-Sγ were refined as single bonds for a good fit with the electron density, with distances of 1.51 and 1.86 Å, respectively. The bond angles around the C4′ atom are 106, 111, and 112°, confirming the tetrahedral geometry of the C4′ atom. The peak shift in the absorption spectrum from 416 to 350 nm observed in the SCL·L-cysteine complex crystal (supplemental Fig. S3*A*) and that in solution (Fig. 2) are thus due to the formation of the tetrahedral adduct of cysteine-PLP-Lys247 (supplemental Fig. S3*D*).

Upon binding of L-cysteine, the small domain moves toward the active site and the extended lobe (small domain residues Ser-374 to Ile-392), which is disordered in the unliganded form, shows its ordered structure, encapsulating L-cysteine within the active site cavity (Figs. 3 and 4*A*). The carboxylate of the bound cysteine makes a salt bridge with the guanidino group of Arg-402 and is further fixed by hydrogen bond interactions with Ser-374 (extended lobe) and Asn-186. The protonated α-amino group of the bound cysteine, which is supposed to form a Schiff base (external aldimine) with PLP in place of Lys-247 in cysteine desulfurases (15, 16), is hydrogen-bonded to the side chain OH group of Ser-374, the main chain C=O group of Ala-26, and water molecule W1.

Structure of SCL·Selenopropionate Complex—We solved the crystal structure of an SCL·selenopropionate complex. Selenopropionate is the substrate analog in which the α-amino group of the substrate L-selenocysteine is replaced by a hydrogen atom. There is no significant difference in the overall and active site fold between selenopropionate and the L-cysteine complex. The residual electron density showed that the bound selenopropionate is disordered over two sites such that the structure is comprised of two conformers, A and B (Fig. 4*B*). Conformer A is just like the bound L-cysteine in SCL·L-cysteine in that the Seγ atom of selenopropionate forms a covalent bond with the C4′ atom of the cofactor, although the distance of 2.28 Å is slightly longer than the normal Se-C bond length (1.98–2.00 Å) (45). The geometry around the C4′ atom is tetrahedral with bond angles of 109, 110, and 113°. On the other hand, conformer B directs its Seγ atom toward the extended lobe and forms a hydrogen bond with the thiol group of the lobe residue Cys-375 (Seγ—Sγ = 3.29 Å) because the selenol group (pK_a of ~5.2) is deprotonated resulting in the selenolato-thiol interaction (46). The Seγ atom further interacts with His-133 NE2 with an interatomic distance of 3.5 Å. The spectrum of SCL measured in solution in the presence of selenopropionate showed peaks at 350 and 416 nm, suggesting that selenopropionate is bound to the active site in the two conformers as observed in the SCL·selenopropionate crystal (supplemental Fig. S4).

DISCUSSION

Catalytic Mechanism—The C375A mutant of SCL does not catalyze the removal of selenium from L-selenocysteine. C375A·L-selenocysteine shows an absorption spectrum that is

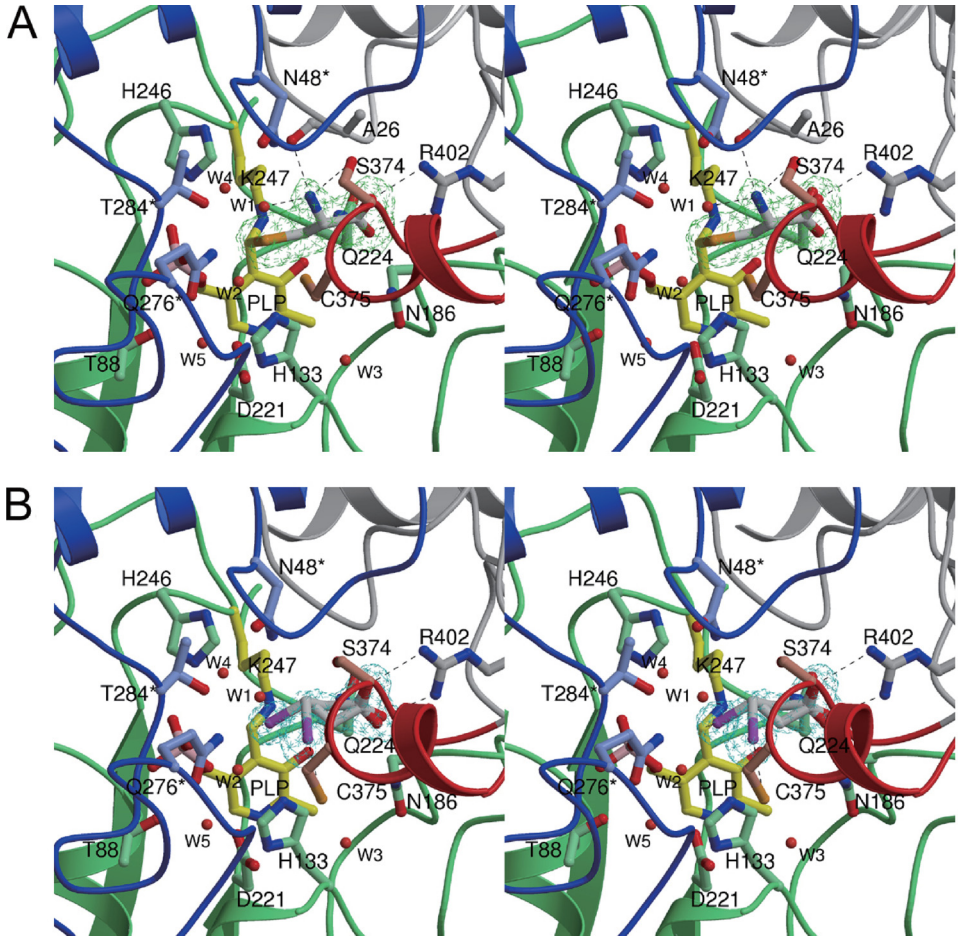

FIGURE 4. **Active site structures.** *A*, SCL complexed with L-cysteine and *B*, SCL complexed with selenopropionate. The PLP moiety, active site residues, and bound ligands (*A*, L-cysteine; *B*, selenopropionate) are shown as *ball-and-stick models*. Water molecules (W1-W5) are presented as *red circles*. Backbone structures of the large domain, the small domain, and the extended lobe in one subunit are drawn in *green*, *gray*, and *red*, respectively. Cα structures and residues (indicated by *asterisks*) in the other subunit of the dimer are shown in *blue*. The $2F_o - F_c$ electron density map contoured at 1.0 σ is calculated from the final model with the bound ligand omitted. Both conformers of selenopropionate are drawn in *B*.

quite similar to that of the SCL·L-cysteine complex (Fig. 2), which suggests that L-selenocysteine forms the tetrahedral adduct with a mutant enzyme, such as L-cysteine bound to the wild-type enzyme. With consideration of the foregoing observations and this fact, we propose that the interaction of the thiol group of Cys-375 with the selenolate of the substrate selenocysteine brings the substrate L-selenocysteine into a favorable arrangement to form a Schiff base with PLP, as was observed in the conformer B of SCL·selenopropionate. SCL is designed to form the productive Michaelis complex by the thiol-selenolate interaction as the guide, although the nonproductive form might be in equilibrium with the productive form.

The productive L-selenocysteine is encapsulated in the active site by a small domain rotation and the ordering of the extended lobe with its Seγ atom interacting with the thiol group of Cys-375. The deprotonated amino group of the substrate makes a nucleophilic attack on the C4′ of PLP to produce the external aldimine and release the neutral side chain of Lys-247. The α-proton of the substrate is eliminated by Lys-247 to yield a quinonoid intermediate. Lys-247 adds a proton to the C4′ of the quinonoid intermediate, producing the substrate-ketimine intermediate. The substrate-ketimine then transfers selenium to Cys-375 to form cysteine selenopersulfide (Cys375-S–Se(H)) and the enamine. Cys-375, which approaches and interacts with the substrate Se atom, plays a critical role in the formation of the selenopersulfide as well as the productive form.

It remains unclear whether selenium is directly released from Cys375-S–Se(H) or trapped by a selenium-transferring protein and subsequently released by a reductant in the reaction system. If selenopersulfide selenium, which is more sensitive to oxygen than persulfide sulfur, is released directly from an intermediate and diluted by the bulk solvent, then delivery to a specific acceptor molecule would be inefficient. Plausibly, selenium is shipped to the target protein through interaction with the selenium-transferring protein in a manner similar to the reaction of cysteine desulfurases (16, 35).

Open-Closed Conformational Change—Cysteine desulfurases thus far determined by x-ray methods exhibit no marked change in their overall or local conformation because the liganded forms have the same structures as those of the unliganded forms (17, 18, 38–40). In contrast, upon binding of L-cysteine or selenocysteine, the disordered extended lobe of SCL in the unliganded form shows its ordered structure composed of the helix 11 (3_{10} helix)–loop- α-helix 12-loop to close the active site in concert with a 3.8° rotation of the small domain as a rigid body (Figs. 3 and 4). The accessible surface area of the bound L-cysteine was calculated to be 0 Å^2, indicating that the open-closed conformational change completely shields bound ligands from the solvent region. The disorder-order transition of the extended lobe is deeply involved in the catalytic event in that the lobe residue Cys-375 is oriented favorably for interaction with the selenol group of the substrate and the oxygen-sensitive selenopersulfide is synthesized in the cavity shielded from the solvent region.

In contrast to SCL, the extended lobe of *E. coli* IscS (38) or the *T. maritima* NifS-like protein (39) (group I cysteine desulfurase) in the unliganded form is only one residue shorter than that of SCL, and is disordered in the region bearing the catalytic cysteine residue (Fig. 3*B*). Upon binding of cysteine to the *T. maritima* NifS-like protein, the lobe remains disordered and does not change its conformation. The accessible surface area of the bound cysteine is 49.3 Å^2. *E. coli* CsdB (group II) has a shorter extended lobe than the group I enzymes. The lobe is ordered and maintains the same

conformation regardless of whether it has the unliganded or liganded form. The accessible surface area of the bound L-propargylglycine is 10.2 Å^2. These results suggest that the ligand bound to group I or II cysteine desulfurase is solvent accessible.

Discrimination between Selenium and Sulfur—Cysteine desulfurases, such as *A. vinelandii* NifS, *E. coli* IscS, and *E. coli* CsdB catalyze the elimination of the Se atom from L-selenocysteine as well as the S atom from L-cysteine (15, 35, 43, 47, 48). On the other hand, SCL is highly specific for L-selenocysteine, as described above and elsewhere (11, 13). UV-visible spectrum analysis and the detailed active site structures of SCL·L-cysteine and SCL·selenopropionate uncovered the molecular basis of the specificity of SCL for L-selenocysteine.

The substrate L-selenocysteine binds to the active site in the productive form with the aid of the interaction of the substrate selenolato with Cys-375 thiol. This interaction allows the substrate to form the Schiff base with PLP resulting in the production of the external aldimine. On the other hand, the bound L-cysteine is not involved in the interaction with the thiol group of Cys-375, but the Sγ atom of the bound L-cysteine makes a covalent bond with the C4′ of PLP to form a stable tetrahedral adduct with the α-amino group far away from the C4′ atom and the Cα-proton directed to the solvent side (Fig. 4*A* and supplemental Fig. S3). Therefore, SCL does not catalyze L-cysteine desulfuration.

SCL acting on selenium but not on its sulfur counterpart is significant among the enzymes participating in selenoprotein biosynthesis: neither selenophosphate synthetase nor selenocysteine synthase shows strict specificity toward selenium compounds (49). Thus, SCL acts as a sorter for selenium from the mixture of selenium and sulfur in a biological system.

Acknowledgments—We thank Dr. Wolfgang Bückel (Max Planck Institute for Terrestrial Microbiology, Marburg), Dr. Rudolf K. Thauer (Max Planck Institute for Terrestrial Microbiology, Marburg), Dr. Roland Lill (Philipps University Marburg, Marburg), and Dr. Antonio J. Pierik (Philipps University Marburg, Marburg) for their kind suggestions concerning this study.

REFERENCES

1. Hatfield, D. L. (2001) *Selenium: Its Molecular Biology and Role in Human Health*, Kluwer Academic Publishers, Norwell, MA
2. Small-Howard, A. L., and Berry, M. J. (2005) *Biochem. Soc. Trans.* **33,** 1493–1497
3. Kim, I. Y., Guimarães, M. J., Zlotnik, A., Bazan, J. F., and Stadtman, T. C. (1997) *Proc. Natl. Acad. Sci. U.S.A.* **94,** 418–421
4. Xu, X. M., Carlson, B. A., Irons, R., Mix, H., Zhong, N., Gladyshev, V. N., and Hatfield, D. L. (2007) *Biochem. J.* **404,** 115–120
5. Carlson, B. A., Xu, X. M., Kryukov, G. V., Rao, M., Berry, M. J., Gladyshev, V. N., and Hatfield, D. L. (2004) *Proc. Natl. Acad. Sci. U.S.A.* **101,** 12848–12853
6. Xu, X. M., Carlson, B. A., Mix, H., Zhang, Y., Saira, K., Glass, R. S., Berry, M. J., Gladyshev, V. N., and Hatfield, D. L. (2007) *PLoS Biol.* **5,** e4
7. Ganichkin, O. M., Xu, X. M., Carlson, B. A., Mix, H., Hatfield, D. L., Gladyshev, V. N., and Wahl, M. C. (2008) *J. Biol. Chem.* **283,** 5849–5865
8. Combs, G. F., Jr., and Combs, S. B. (1984) *Annu. Rev. Nutr.* **4,** 257–280
9. Schwarz, K. (1965) *Fed. Proc.* **24,** 58–67
10. Esaki, N., Nakamura, T., Tanaka, H., Suzuki, T., Morino, Y., and Soda, K. (1981) *Biochemistry* **20,** 4492–4496
11. Esaki, N., Nakamura, T., Tanaka, H., and Soda, K. (1982) *J. Biol. Chem.* **257,** 4386–4391
12. Chocat, P., Esaki, N., Tanizawa, K., Nakamura, K., Tanaka, H., and Soda, K. (1985) *J. Bacteriol.* **163,** 669–676
13. Mihara, H., Kurihara, T., Watanabe, T., Yoshimura, T., and Esaki, N. (2000) *J. Biol. Chem.* **275,** 6195–6200
14. Grishin, N. V., Phillips, M. A., and Goldsmith, E. J. (1995) *Protein Sci.* **4,** 1291–1304
15. Mihara, H., Kurihara, T., Yoshimura, T., and Esaki, N. (2000) *J. Biochem.* **127,** 559–567
16. Zheng, L., White, R. H., Cash, V. L., and Dean, D. R. (1994) *Biochemistry* **33,** 4714–4720
17. Fujii, T., Maeda, M., Mihara, H., Kurihara, T., Esaki, N., and Hata, Y. (2000) *Biochemistry* **39,** 1263–1273
18. Lima, C. D. (2002) *J. Mol. Biol.* **315,** 1199–1208
19. Smith, A. D., Frazzon, J., Dean, D. R., and Johnson, M. K. (2005) *FEBS Lett.* **579,** 5236–5240
20. Kambampati, R., and Lauhon, C. T. (2000) *J. Biol. Chem.* **275,** 10727–10730
21. Ikeuchi, Y., Shigi, N., Kato, J., Nishimura, A., and Suzuki, T. (2006) *Mol. Cell* **21,** 97–108
22. Ollagnier-de-Choudens, S., Lascoux, D., Loiseau, L., Barras, F., Forest, E., and Fontecave, M. (2003) *FEBS Lett.* **555,** 263–267
23. Outten, F. W., Wood, M. J., Munoz, F. M., and Storz, G. (2003) *J. Biol. Chem.* **278,** 45713–45719
24. Mueller, E. G. (2006) *Nat. Chem. Biol.* **2,** 185–194
25. Esaki, N., and Soda, K. (1987) *Methods Enzymol.* **143,** 415–418
26. Mihara, H., and Esaki, N. (2002) *Methods Enzymol.* **347,** 198–203
27. Matthews, B. W. (1968) *J. Mol. Biol.* **33,** 491–497
28. Otwinowski, Z., and Minor, W. (1997) *Methods Enzymol.* **276,** 307–326
29. Navaza, J., and Saludjian, P. (1997) *Methods Enzymol.* **276,** 581–594
30. Jones, T. A., Zou, J. Y., Cowan, S. W., and Kjeldgaard, M. (1991) *Acta Crystallogr. A* **47,** 110–119
31. Brünger, A. T., Adams, P. D., Clore, G. M., DeLano, W. L., Gros, P., Grosse-Kunstleve, R. W., Jiang, J. S., Kuszewski, J., Nilges, M., Pannu, N. S., Read, R. J., Rice, L. M., Simonson, T., and Warren, G. L. (1998) *Acta Crystallogr. D Biol. Crystallogr.* **54,** 905–921
32. Kraulis, P. J. (1991) *J. Appl. Crystallogr.* **24,** 946–950
33. Fenn, T. D., Ringe, D., and Petsko, G. A. (2003) *J. Appl. Crystallogr.* **36,** 944–947
34. DeLano, W. L. (2001) *The PyMOL Molecular Graphics System*, DeLano Scientific, San Carlos, CA
35. Mihara, H., and Esaki, N. (2002) *Appl. Microbiol. Biotechnol.* **60,** 12–23
36. Mehta, P. K., Hale, T. I., and Christen, P. (1993) *Eur. J. Biochem.* **214,** 549–561
37. Holm, L., and Sander, C. (1993) *J. Mol. Biol.* **233,** 123–138
38. Cupp-Vickery, J. R., Urbina, H., and Vickery, L. E. (2003) *J. Mol. Biol.* **330,** 1049–1059
39. Kaiser, J. T., Clausen, T., Bourenkow, G. P., Bartunik, H. D., Steinbacher, S., and Huber, R. (2000) *J. Mol. Biol.* **297,** 451–464
40. Tirupati, B., Vey, J. L., Drennan, C. L., and Bollinger, J. M., Jr. (2004) *Biochemistry* **43,** 12210–12219
41. Clausen, T., Kaiser, J. T., Steegborn, C., Huber, R., and Kessler, D. (2000) *Proc. Natl. Acad. Sci. U.S.A.* **97,** 3856–3861
42. Momany, C., Levdikov, V., Blagova, L., Lima, S., and Phillips, R. S. (2004) *Biochemistry* **43,** 1193–1203
43. Mihara, H., Kurihara, T., Yoshimura, T., Soda, K., and Esaki, N. (1997) *J. Biol. Chem.* **272,** 22417–22424
44. Mihara, H., Fujii, T., Kato, S., Kurihara, T., Hata, Y., and Esaki, N. (2002) *J. Biochem.* **131,** 679–685
45. Allen, F. H., Watson, D. G., Brammer, L., Orpen, A. G., and Taylor, R. (1999) in *International Tables for Crystallography* (Wilson, A. J. C., and Prince, E., eds) Vol. C, pp. 782–803, Kluwer Academic Publishers, Dordrecht, The Netherlands
46. Ursini, F., and Bindoli, A. (1987) *Chem. Phys. Lipids* **44,** 255–276
47. Zheng, L., White, R. H., Cash, V. L., Jack, R. F., and Dean, D. R. (1993) *Proc. Natl. Acad. Sci. U.S.A.* **90,** 2754–2758
48. Mihara, H., Maeda, M., Fujii, T., Kurihara, T., Hata, Y., and Esaki, N. (1999) *J. Biol. Chem.* **274,** 14768–14772
49. Tormay, P., Wilting, R., Lottspeich, F., Mehta, P. K., Christen, P., and Böck, A. (1998) *Eur. J. Biochem.* **254,** 655–661